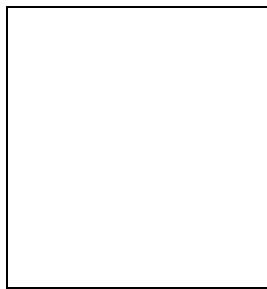


HIGH PRECISION LASER AND MICROWAVE SPECTROSCOPY OF ANTIPROTONIC HELIUM

E. WIDMANN

for the ASACUSA collaboration

Department of Physics, University of Tokyo, 7-3-1 Hongo, Bunkyo-ku, Tokyo 113-0011, Japan



This talk gives an overview of the recent results on the precision spectroscopy of antiprotonic helium which was performed by the ASACUSA collaboration at the Antiproton Decelerator of CERN. The laser spectroscopy of energy levels of the antiproton has reached a relative accuracy of $\sim 10^{-7}$, and by comparing the experimental value for the transition wavelengths with theoretical calculations, a CPT test on the equality of proton and antiproton charge and mass of $< 6 \times 10^{-8}$ has been obtained. In a recent experiment, the hyperfine structure of the $(n, l) = (37, 35)$ state of antiprotonic helium has been measured for the first time with an accuracy of 3×10^{-5} .

1 Antiprotonic helium

The precision spectroscopy of antiprotonic helium is being performed by the ASACUSA collaboration¹ at the Antiproton Decelerator (AD) facility of CERN in Geneva, Switzerland. The experiments constitute an extension of those performed previously by the PS205 collaboration at LEAR^{2,3,4}. Here, highly excited states of the neutral three-body system $\bar{p}\text{-He}^{2+}\text{-e}^- \equiv \bar{p}\text{He}^+$ (cf. Fig. 1) are investigated by means of laser and microwave spectroscopy. These states are formed when antiprotons are stopped in helium (in the current experiments, helium gas of about 6 K and 0.1 – 2 bar). Antiprotons are captured by replacing one of the two ground-state electrons of helium and therefore occupy states with principal quantum numbers around $n_0 = \sqrt{M^*/m}$ ($=38.3$ for $\bar{p}^4\text{He}^+$), where M^* is the reduced mass of the $\bar{p}\text{-He}^{2+}$ system, and m the electron mass. Fig. 1 shows the energy level diagram of $\bar{p}^4\text{He}^+$, which is divided in a metastable zone (solid lines) and a short-lived one (wavy lines). For the metastable levels the Auger transition rate is much smaller than the radiative transition rate, leading to lifetimes of $\tau \sim \mu\text{s}$, while for the short-lived ones the Auger rate is much higher than the radiative one, resulting in lifetimes of $\tau < 10$ ns. Antiprotons initially captured around n_0 undergo radiative transitions following

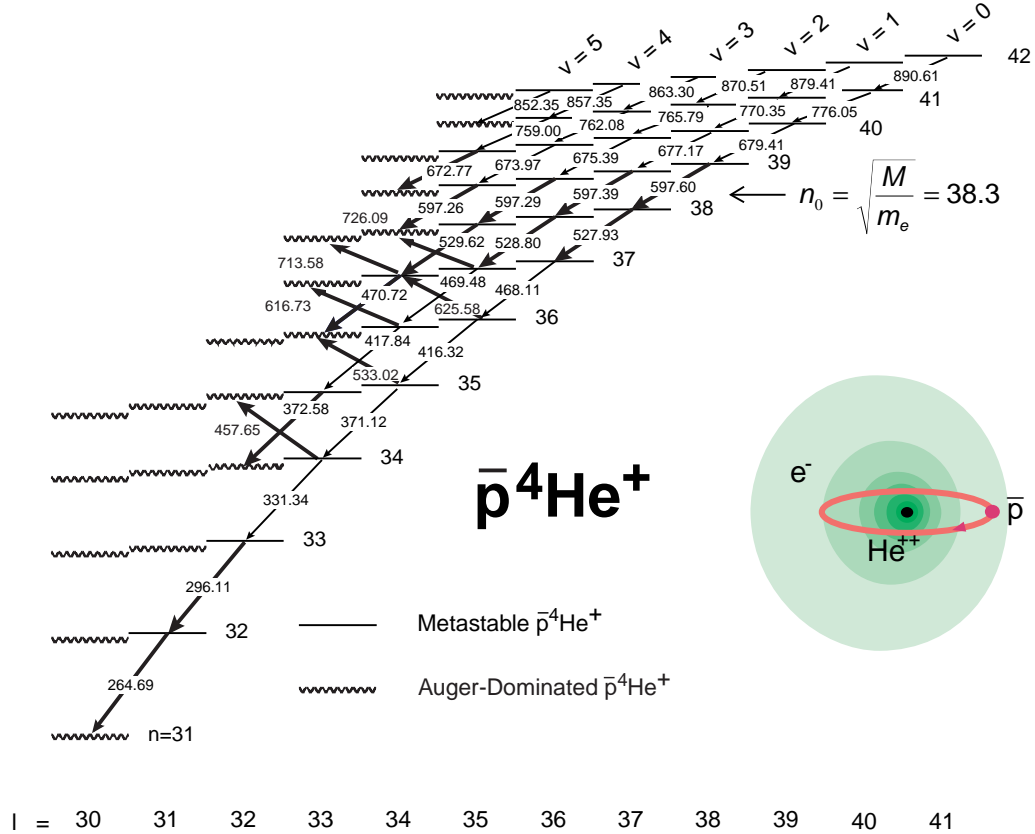


Figure 1: Right: structure of antiprotonic helium. Left: Energy level diagram of $\bar{p}^4\text{He}^+$. Metastable levels ($\tau \geq \mu\text{s}$) are denoted by solid lines, Auger-dominated short-lived ones ($\tau \leq 10 \text{ ns}$) by wavy lines. Arrows symbolize radiative transitions following the propensity rule $\Delta v = 0$. Bold arrows correspond to experimentally observed transitions. They include so-called unfavoured ones with $\Delta v = 2$. The transition wavelengths are denoted in units of nm.

cascades with $\Delta v \equiv \Delta(n - l - 1) = 0$ ($n =$ principle and $l =$ angular momentum quantum number) until they reach a short-lived state from which they ionize via Auger transitions. The $\bar{p}\text{He}^{++}$ ion is then rapidly destroyed by Starck-mixing in the dense surrounding helium medium.

This picture was proven to be correct by a series of laser spectroscopy experiments at LEAR (5 and references in 4). A laser pulse tuned to the transition at the end of a cascade will deexcite the antiprotons from the metastable to the short-lived state, thus forcing them to immediately annihilate. Using this signature, a total of 10 resonant transitions in $\bar{p}^4\text{He}^+$ and 3 in $\bar{p}^3\text{He}^+$ could be found at LEAR, thus confirming for the first time experimentally the long-held belief that exotic particles are initially captured around $n_0 = \sqrt{M^*/m}$.

2 Laser spectroscopy of antiprotonic helium and CPT test of the antiproton charge and mass

The AD is in operation since the year 2000. It provides pulses of $\sim 200 \text{ ns}$ length containing $2-4 \times 10^7$ antiprotons of $100 \text{ MeV}/c$ momentum (5.3 MeV kinetic energy). The distance between pulses is about 100 seconds. For the experiments at the AD a completely new experimental setup was designed and installed, adopted to the pulsed structure of the antiproton beam with very low repetition rate. Laser spectroscopy of $\bar{p}\text{He}^+$ was started from the begin of operation of the AD, and many new transitions in $\bar{p}^4\text{He}^+$ and $\bar{p}^3\text{He}^+$ were found. This allows for a much more systematic study of state properties and theoretical calculations.

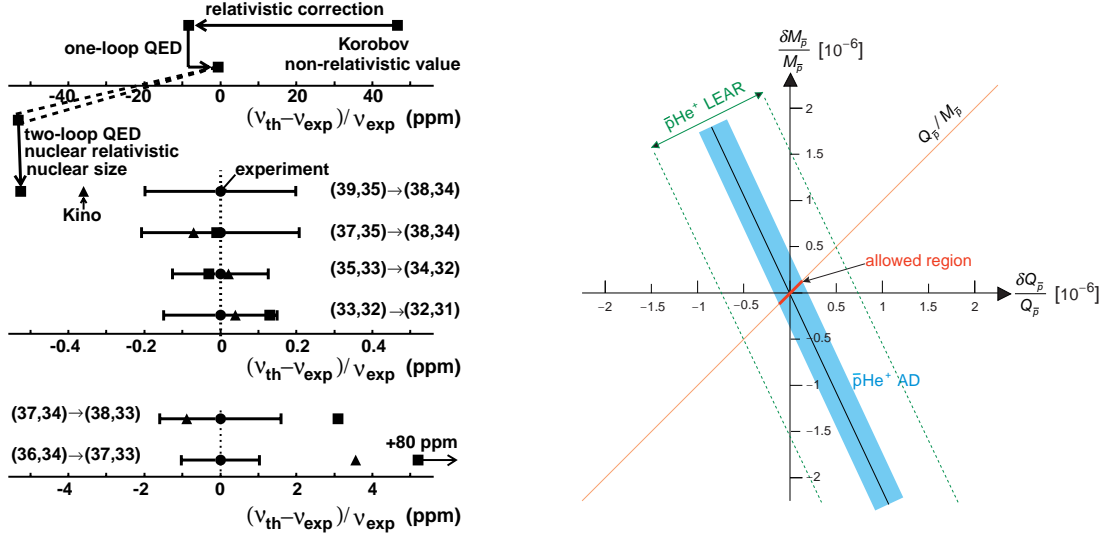


Figure 2: Left: Comparisons between experimental (filled circles with errors) and theoretical (squares⁸ and triangles^{9,10}) values for six transition frequencies in $\bar{p}\text{He}^+$ atoms. The upper four “narrow” (see text) transitions show agreement between theory and experiment to better than 5×10^{-7} . Right: Two-dimensional constraint on the relative deviation of the proton and antiproton charge and mass obtained from the cyclotron frequency of the antiproton¹¹ and from the spectroscopic studies of $\bar{p}\text{He}^+$ at LEAR⁶ and at the AD⁷.

At LEAR, we had succeeded in measuring the transition wavelength for one transition with the best accuracy of 0.5 ppm (5×10^{-7})⁶. In order to improve this, we used a new laser system and more sophisticated calibration of the wavelength measuring device against an iodine reference cell⁷. In the first experiment, we also extended the measurements to six transitions including two newly found ones in the UV region ($(n, l) = (35, 33) \rightarrow (34, 32)$ at 372 nm and $(33, 32) \rightarrow (32, 31)$ at 296 nm) where theoretical calculations are supposed to be most accurate. Two transitions had very large widths ($\Gamma > 15$ GHz) because of the short lifetime of their daughter states, which makes both the experimental and theoretical accuracy very low. For the other four “narrow” transitions ($\Gamma < 50$ MHz), the experimental error was reduced by a factor of four to 1.3×10^{-7} , and all four transition wavelengths agreed with the most sophisticated three-body calculations by Korobov⁸ and Kino et al.^{9,10} to better than 5×10^{-7} (cf. Fig. 2)⁷. At this level of precision the calculations need to take into account relativistic corrections, the Lamb shift and QED corrections up to order α^4 , so that this experiment constitutes a stringent test of the validity of three-body bound state QED calculations.

On the other hand, the agreement between experiment and theory can be used to perform a CPT test on the proton/antiproton charge and mass, since the theorists use in their calculations the numerically better known mass and charge of the proton. The energy levels itself are governed by the Rydberg constant $Ry \sim M_{\bar{p}} Q_{\bar{p}}^2$. Taking into account the fact that the antiproton cyclotron frequency $\omega_{\bar{p}} \sim Q_{\bar{p}}/M_{\bar{p}}$ is known¹¹ to be equal to the proton one to better than 1 in 10^{10} , the agreement of theory and experiment for the transition energies in antiprotonic helium results in an upper limit for the equality of proton and antiproton charge and mass of 6×10^{-8} (90% confidence level)⁷, a factor of 8 better than our own results at LEAR⁶ and a factor of 300 better than previous measurements using X-rays of heavy antiprotonic atoms¹².

In 2001 we went one step ahead and used an Radio Frequency Quadrupole Decelerator (RFQD¹³) to further decelerate the antiprotons to ~ 60 keV. These ultra-low energy antiprotons can be stopped in helium gas of 30 K and 0.8 mbar, about a factor 1000 lower density than usual. This allows to essentially eliminate the systematic error coming from the extrapolation of the transition wavelength to zero density necessary in the previous experiments. Furthermore, we extended the number of transitions investigated to 7 in $\bar{p}^4\text{He}^+$ and, for the first time, included

6 transitions of $\bar{p}^3\text{He}^+$. Preliminary analysis shows that we can expect a further improvement of a factor 3...4 for the experimental accuracy after analyzing all new data.

3 Measurement of the hyperfine structure of antiprotonic helium

The main highlight of the 2001 run was the first observation of the hyperfine splitting of the (37,35) state using a laser-microwave-laser triple resonance method¹⁴. In this case “hyperfine” structure means the level splitting arising from the interaction of the magnetic moments of the constituents of $\bar{p}\text{He}^+$. The uniqueness of the resulting structure comes from the fact that the antiproton in metastable states carries a very large angular momentum of $L_{\bar{p}} = 33 \dots 39$, which leads through the interaction $\vec{L}_{\bar{p}} \cdot \vec{S}_e$ with the electron spin S_e to the dominant splitting which we call *hyperfine (HF)* splitting. The antiproton spin $S_{\bar{p}}$ leads to a further, about two orders of magnitude smaller splitting called *super-hyperfine (SHF)* structure, resulting in a quadruplet structure (cf. Fig. 3).

The two-laser microwave triple resonance method¹⁴ allows to observe the transitions ν_{HF}^+ and ν_{HF}^- within the quadruplet that are associated with a flip of the *electron* spin. The measured values agree well with the calculated ones by Korobov and Bakalov^{15,16}, but less with published values of Yamanaka and Kino¹⁷. New results of Kino et al.¹⁰, however, are very close to our experimental results. The experiment has therefore fully confirmed the presence of a quadruplet structure originating from the hyperfine coupling of $\vec{L}_{\bar{p}}$, \vec{S}_e , and $\vec{S}_{\bar{p}}$, as predicted by Bakalov and Korobov¹⁵. The latest values of both theoretical groups agree with our result on the level of the theoretical accuracy which is determined from omitting order- $\alpha^2 \approx 5 \times 10^{-5}$ corrections from the calculations. This again shows the impressive accuracy that the variational three-body QED calculations are able to achieve. The experimental accuracy is $\sim 3 \times 10^{-5}$, slightly smaller than the theoretical uncertainty.

The excellent agreement between experiment and theory proves the validity of the theoretical expressions of Bakalov and Korobov for the HFS of $\bar{p}\text{He}^+$. The microwave resonance frequencies, ν_{HF}^+ and ν_{HF}^- , are primarily related to the dominant \bar{p} orbital magnetic moment. On the other hand, the splitting between ν_{HF}^+ and ν_{HF}^- is caused by the \bar{p} spin, and is directly proportional to the spin-magnetic moment $\mu_{\bar{p}}$ of the antiproton. The observation of a splitting in agreement with the theoretical value implies that the spin-magnetic moment of proton and antiproton are equal within the experimental error of 1.6 %. This is consistent with an earlier (more precise) determination of $\mu_{\bar{p}}$ from a fine structure measurement of antiprotonic lead¹⁸.

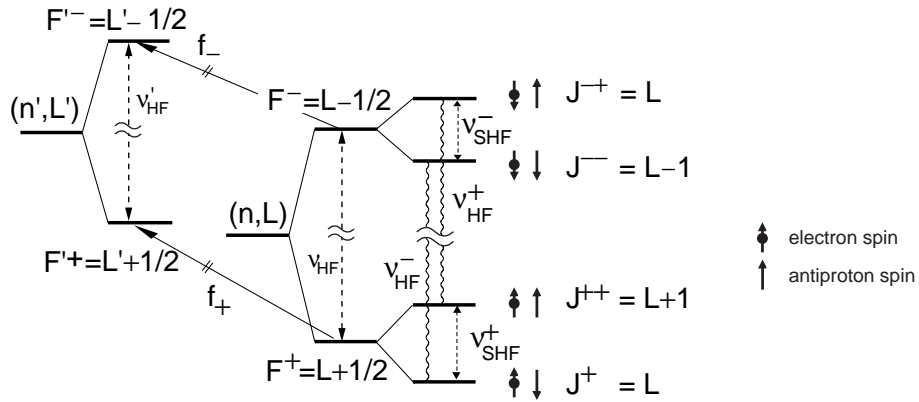


Figure 3: Schematic view of the splitting of a $\bar{p}\text{He}^+$ state and observable laser transitions from the F^\pm levels of a (n, L) state to a daughter state (n', L') (arrows). Wavy lines denote allowed magnetic transitions associated with an electron spin flip.

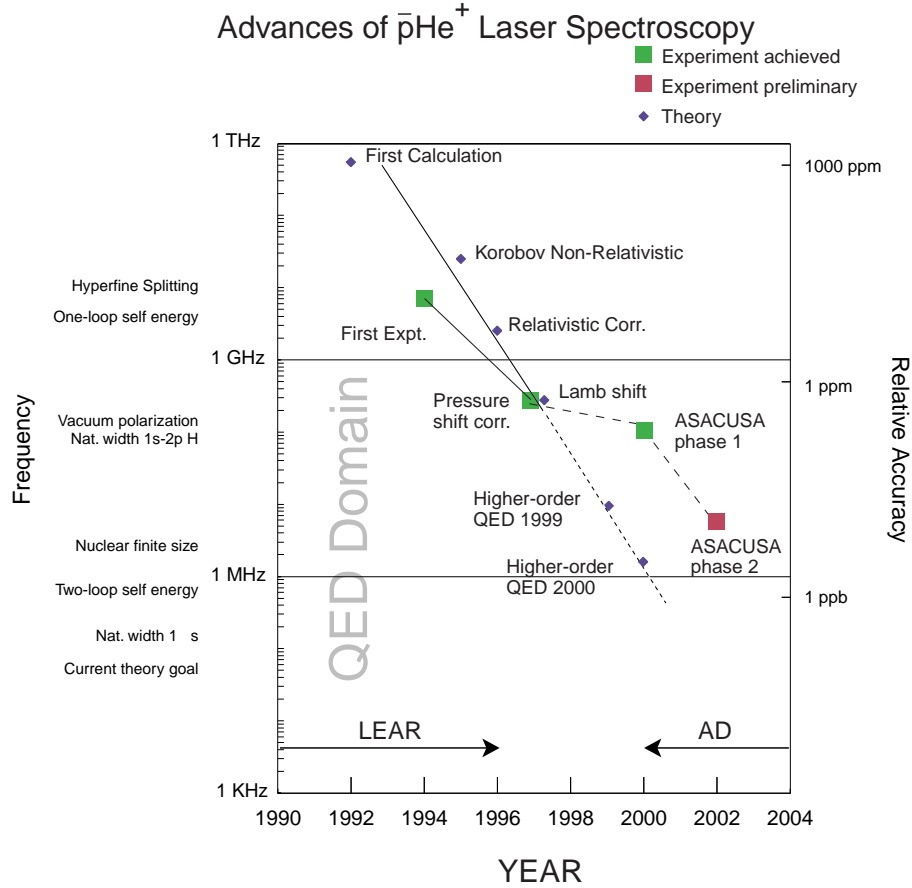


Figure 4: Evolution of both experimental and theoretical accuracy for laser spectroscopy of $\bar{p}\text{He}^+$.

4 Summary and Outlook

Fig. 4 illustrates the development of the laser spectroscopy measurements as well as the theoretical calculations over the years. It shows a step-by-step progress, in which an advance of experiments was followed by an improvement of the theoretical calculations, which was repeated several times. The experimental results provided the grounds for an advancement of three-body QED calculations to a precision that has never been reached before for a three-body system with two heavy centers (antiproton and helium nucleus). The agreement between theory and experiment could be used to perform a CPT test on the equivalence of proton and antiproton charge and mass with an accuracy of 60 ppb, which will be improved by a factor 3...4 in the near future. Making use of the ultra-low energy antiproton beam provided by the ASACUSA RFQD, and two-photon transitions with a new laser system currently under development, we expect to increase the experimental precision by about another order of magnitude in the next two years.

The first measurement of microwave-induced transitions within a state in $\bar{p}\text{He}^+$ proves its unusual hyperfine structure due to the large angular momentum of the antiproton. The agreement with theory provides a measurement of the orbital angular momentum of \bar{p} with an accuracy of 6×10^{-5} . The value for the spin magnetic moment agrees with earlier (more precise) measurements. An improvement of the accuracy of one order of magnitude is necessary to improve the value for $\mu_{\bar{p}}$, which is known to only 0.3%.

1. ASACUSA collaboration, Atomic spectroscopy and collisions using slow antiprotons, CERN/SPSC 97-19, CERN/SPSC 2000-04 (1997/2000).
2. M. Iwasaki *et al.*, *Phys. Rev. Lett.* **67**, 1246 (1991).
3. T. Yamazaki *et al.*, *Nature* **361**, 238 (1993).
4. T. Yamazaki, N. Morita, R. S. Hayano, E. Widmann and J. Eades, *Phys. Rep.* **366**, 183 (2002).
5. N. Morita *et al.*, *Phys. Rev. Lett.* **72**, 1180 (1994).
6. H. A. Torii *et al.*, *Phys. Rev. A* **59**, 223 (1999).
7. M. Hori *et al.*, *Phys. Rev. Lett.* **87**, 093401 (2001).
8. V. I. Korobov, *Nucl. Phys. A* **684**, 663c (2001), *Nucl. Phys. A* 689(2001) 75c.
9. Y. Kino, M. Kamimura and H. Kudo, *Hyperfine Interactions* **119**, 201 (1999).
10. Y. Kino, N. Yamanaka, M. Kamimura and H. Kudo, in: Proceedings of the 3rd European Conference on Atomic Physics at Accelerators (APAC2001), Hyperfine Interactions, in press, Aarhus, Denmark, 2001.
11. G. Gabrielse *et al.*, *Phys. Rev. Lett.* **82**, 3198 (1999).
12. D. Groom *et al.*, *The European Physical Journal C* **15**, 1 (2000).
13. J. Bossler *et al.*, Feasibility study of a decelerating radio frequency quadrupole system for the antiproton decelerator AD, CERN PS/HP Note 97-36 (1997).
14. E. Widmann *et al.* *Physical Review Letters*, in print.
15. D. Bakalov and V. I. Korobov, *Phys. Rev. A* **57**, 1662 (1998).
16. V. Korobov and D. Bakalov, *J. Phys. B: At. Mol. Opt. Phys.* **34**, L519 (2001).
17. N. Yamanaka, Y. Kino, H. Kudo and M. Kamimura, *Phys. Rev. A* **63**, 012518 (2000).
18. A. Kreissl *et al.*, *Z. Phys. C* **37**, 557 (1988).